

DESIGN OF CONSTRAINED KALMAN FILTER FOR THE ESTIMATION OF SIGNAL AND IMAGE PARAMETERS

Md Saifur Rahman

System LSI Division

Samsung Electronics, Bangalore, India.

Abstract: Kalman filtering is an extensively used technique to estimate the states of discrete-time dynamic systems in a wide range of applications. However, in the application of Kalman filters some known signal information like, state variable constraints which may be based on physical considerations are often neglected because they do not fit easily into the structure of the Kalman filter. The negligence of the state variable constraints sometimes leads to inaccurate estimation. Even worse, the filter may diverge under poor initial conditions. This paper presents a new technique to incorporate state inequality constraints in the traditional Kalman filter. The constraints may be any of linear or nonlinear and time varying or invariant. Logarithmic barrier functions are used to enforce these constraints which improve, significantly, the prediction accuracy and convergence speed of the filter. The performance of this algorithm has been tested for frequency and phasor estimation of a noisy sinusoid and, for yawn detection in human drivers by estimating the lip motion.

Key Words: Kalman Filter, State Constraints, Logarithmic Barrier Function, Signal Parameter Estimation, Yawn Detection, Lip Motion Estimation.

1. Introduction

The Kalman filter (KF) is a set of mathematical equations [1] that provides an efficient computational means to estimate the state of a process, in a way that minimizes the mean of the squared error. The filter is very powerful in several aspects: it supports estimations of past, present, and even future states, and it can do so even when the precise nature of the modeled system is unknown. KF has been applied in areas as diverse as communication, biomedical, seismology, navigation, aerospace, and radar and sonar technologies. However, in the application of Kalman filters some known signal information like, state variable constraints which may be based on physical considerations are often neglected because they do not fit easily into the structure of the Kalman filter. Without the constraints a normal KF at times may diverge and generate wayward estimates of the states. People have been working in the area of constrained KF and have proposed several ways to handle the constraints. Some researchers treated state constraints by reducing the system model parameterization [2, 3]. Some treated constraints as perfect measurements [4, 5]. Simon and Chia proposed

an alternative method [6], which incorporates the state constraints into the state estimation framework by projecting the unconstrained KF solution onto the constraint surface at each time step.

In this paper the traditional KF is generalized in such a way that the known state inequality constraints are satisfied by the state variable estimates. Logarithmic Barrier Functions [7] are used to enforce these constraints. A modified and augmented state estimation error vector is obtained by adding two terms, based on Logarithmic Barrier Functions corresponding to every state with the estimation error. The trace of the error covariance matrix of the augmented estimation error vector is minimized to get the Constrained Kalman Filter (CKF) equations. The performance of CKF has been tested for frequency and phasor estimation of a noisy sinusoid and, for lip motion estimation to detect yawn in human drivers. CKF exhibits superior performance over unconstrained KF with respect to estimation accuracy and convergence speed. The paper contains four sections. Traditional KF algorithm has been presented in section 2. The details of the proposed CKF and its performance have been discussed in section 3.

2. Unconstrained KF

Linear Kalman Filter: The Linear KF addresses the general problem of trying to estimate the state $X_k \in R^n$ of a discrete-time process that is governed by the linear stochastic difference equation with a measurement $Y_k \in R^m$,

$$\text{Process:} \quad X_{k+1} = AX_k + BU_k + m_k \quad (1)$$

$$\text{Measurement:} \quad Y_k = CX_k + DU_k + n_k \quad (2)$$

where,

A, B, C and D are matrices of appropriate dimensions

U_k = control input vector

m_k = process noise vector

n_k = measurement noise vector

Assuming Q and R to be process and measurement noise covariance matrices, Linear KF equations are given by,

$$\hat{X}_k^- = A\hat{X}_{k-1} + BU_{k-1} \quad (3)$$

$$P_k^- = AP_{k-1}A^T + Q \quad (4)$$

$$G_k = P_k^- C^T (CP_k^- C^T + R)^{-1} \quad (5)$$

$$\hat{X}_k = \hat{X}_k^- + G_k (Y_k - C\hat{X}_k^- - DU_k) \quad (6)$$

$$P_k = (I - G_k C) P_k^- \quad (7)$$

where,

\hat{X}_k^- = predicted state vector

\hat{X}_k = estimated state vector

P_k^- = predicted error covariance matrix

P_k = estimated error covariance matrix

G_k = Kalman gain matrix

Extended Kalman Filter: Let us assume that our process again has a state vector $X_k \in R^n$, it is now governed by the non-linear stochastic difference equation,

$$\text{Process: } X_{k+1} = f(X_k) + BU_k + m_k \quad (8)$$

$$\text{Measurement: } Y_k = g(X_k) + DU_k + n_k \quad (9)$$

where, f and g are some nonlinear functions. Extended KF algorithm can be written as,

$$\hat{X}_k^- = f(\hat{X}_{k-1}) + BU_{k-1} \quad (10)$$

$$P_k^- = \left(\frac{\delta f(\hat{X}_{k-1})}{\delta X} \right) P_{k-1} \left(\frac{\delta f(\hat{X}_{k-1})}{\delta X} \right)^T + Q \quad (11)$$

$$G_k = P_k^- \left(\frac{\delta g(\hat{X}_k^-)}{\delta X} \right)^T \left(\left(\frac{\delta g(\hat{X}_k^-)}{\delta X} \right) P_k^- \left(\frac{\delta g(\hat{X}_k^-)}{\delta X} \right)^T + R \right)^{-1} \quad (12)$$

$$\hat{X}_k = \hat{X}_k^- + G_k (Y_k - g(\hat{X}_k^-) - DU_k) \quad (13)$$

$$P_k = \left(I - G_k \left(\frac{\delta g(\hat{X}_k^-)}{\delta X} \right) \right) P_k^- \quad (14)$$

3. Constrained KF

3.1 Barrier Method: Consider the optimization problem, $\min f(x)$ subject to $f_i(x) < 0, i = 1, \dots, m$ (15)

We can rewrite the problem as,

$$\min f(x) + (1/t)I(x) \quad (16)$$

where, t is some scale factor and Function $I(x)$ has the following properties:

1. $I(x)$ is convex, with continuous second derivatives

2. $\text{dom } I(x) = \{x \mid f_i(x) < 0, i = 1, \dots, m\}$

3. If $z_k \rightarrow \text{bd } \text{dom } I(x)$, then $I(z_k) \rightarrow \infty$

We refer to such a function as a barrier function for the problem (15). The most widely used barrier function is the logarithmic barrier, defined as

$$I(x) = -\sum_{i=1}^m \log(-f_i(x)) \quad (17)$$

In this paper, logarithmic barrier functions are used to enforce state inequality constraints.

3.2 Signal Parameter Estimation

Problem Definition: A sampled noisy sinusoidal signal can be written as:

$$y_k = A \cos(k\omega T_s + \phi) + \varepsilon_k \quad (18)$$

$$= F(X_k) + \varepsilon_k$$

where,

T_s = sampling time,

$X_k(1) = A$ = amplitude,

$X_k(2) = \omega$ = frequency in radian/sec,

$X_k(3) = \phi$ = phase in radian.

ε_k = zero-mean Gaussian additive white noise

Our objective is to accurately estimate the amplitude, frequency and phase of the noisy sinusoid in the presence of linear, and time invariant state inequality constraints.

Design of CKF: A noisy sinusoid of (18) can be represented in a non-linear state space model as follows:

$$\text{Process: } X_{k+1} = X_k + m_k \quad (19)$$

$$\text{Measurement: } y_k = F(X_k) + \varepsilon_k \quad (20)$$

Linear and time invariant state inequality constraints are given as,

$$X_L < \hat{X}_k < X_H \quad (21)$$

where, X_L and X_H are the lower and the upper bound on the state vector X_k and \hat{X}_k is its estimate. We define the error in estimation of i^{th} state variable at k^{th} time instant as follow,

$$u_k^i = t(x_k^i - \hat{x}_k^i) - g(x_k^i) \quad (22)$$

where, t = scaling factor and logarithmic barrier function

$$g(x_k^i) = \log(x_k^i - x_L^i) + \log(x_H^i - x_k^i)$$

First order Taylor's series expansion about a priori estimate, \hat{x}_k^{i-} gives,

$$\log(x_k^i - x_L^i) = \log(\hat{x}_k^{i-} - x_L^i) + \frac{1}{(\hat{x}_k^{i-} - x_L^i)} (x_k^i - \hat{x}_k^{i-})$$

$$\log(x_H^i - x_k^i) = \log(x_H^i - \hat{x}_k^{i-}) - \frac{1}{(x_H^i - \hat{x}_k^{i-})} (x_k^i - \hat{x}_k^{i-})$$

Therefore,

$$g(x_k^i) = \log(x_k^i - x_L^i) + \log(x_H^i - x_k^i)$$

$$= \overbrace{\log(\hat{x}_k^{i-} - x_L^i) + \log(x_H^i - \hat{x}_k^{i-})}^{Y_k^i}$$

$$+ \overbrace{\left[\frac{1}{(\hat{x}_k^{i-} - x_L^i)} - \frac{1}{(x_H^i - \hat{x}_k^{i-})} \right]}^{Z_k^i} (x_k^i - \hat{x}_k^{i-})$$

$$= Y_k^i + Z_k^i e_k^{i-} \quad (23)$$

where, $e_k^{i-} = (x_k^i - \hat{x}_k^{i-})$, a priori estimation error

$e_k^i = (x_k^i - \hat{x}_k^i)$, posteriori estimation error

Hence, the *augmented* state estimation error vector is:

$$u_k = te_k + Y_k + Z_k e_k^- \quad (24)$$

where, $Y_k = (Y_k^1, Y_k^2, \dots, Y_k^N)^T$

$$Z_k = \text{diag}(Z_k^1, Z_k^2, \dots, Z_k^N)$$

Minimizing the trace of the error covariance matrix, $P_k = E(u_k u_k^T)$ with respect to Kalman Gain, G_k we get recursive CKF algorithm as follows:

$$P_k^- = P_{k-1}, \hat{X}_k^- = \hat{X}_{k-1} \quad (25)$$

$$K_k = \left. \frac{\partial F}{\partial X_k} \right|_{X_k = \hat{X}_k^-} \quad (26)$$

$$G_{k,unc} = P_k^- K_k^T (K_k P_k^- K_k^T + R_k)^{-1} \quad (27)$$

$$G_k = \left(I - \frac{Z_k}{t} \right) G_{k,unc} \quad (28)$$

$$P_k = (I - G_k K_k) P_k^- \quad (29)$$

$$\hat{X}_k = \hat{X}_k^- + G_k (y_k - F(\hat{X}_k^-)) \quad (30)$$

where, $G_{k,unc}$ is the unconstrained Kalman Gain.

Selection of scaling parameter (t): t should not be very small nor should it be too large. In most of the cases $t = 1$ serves as a good starting value. After every iteration, t is updated as $t = \mu t$ where μ is a positive number, greater than one.

Performance Analysis:

Estimation of parameters of synthetic noisy signal:

The Performance of the CKF was tested on a synthetic noisy signal with SNR = 30 dB. Amplitude, frequency and phase were taken to be 1, 50 Hz and 0.2π radians, respectively. The sampling frequency was maintained at 1 kHz. The performance of CKF was compared with unconstrained KF. Simulations were done with same initial values for the both filters. The lower and upper bounds of the inequality constraints were taken as 0 and 1.5 for the amplitude, 45 Hz and 55 Hz for the frequency and 0 radian and π radian for phase. The comparative simulation results are shown in Fig. 1. Compared to the estimation of frequency and phase, amplitude estimation is achieved in less number of iterations. The reasons for faster estimation of amplitude in either case can be ascribed to the dependency of the frequency and phase on the additive noise which is non-linear by nature. The superior performance of CKF is apparent from Fig. 1.

Estimation of parameters of real world signal:

A low frequency real world signal was obtained from 3-phase AC alternator. Amplitude and frequency of the signal were proportional to the speed of the rotor shaft. CKF was applied to estimate signal amplitude, frequency and phase corresponding to a particular shaft speed. Estimation results are shown in Fig. 2. The estimated amplitude, frequency and phase are 0.765, 19.2 Hz and 0.74 radian, respectively. The constraints on the amplitude, frequency and phase are obtained from the practical considerations. Since the speed of the motor shaft is limited to the mechanical limit, amplitude constraints are chosen to be 0 in the lower side and 1.0 in the higher side. The phase constraints are kept at $-\pi/2$

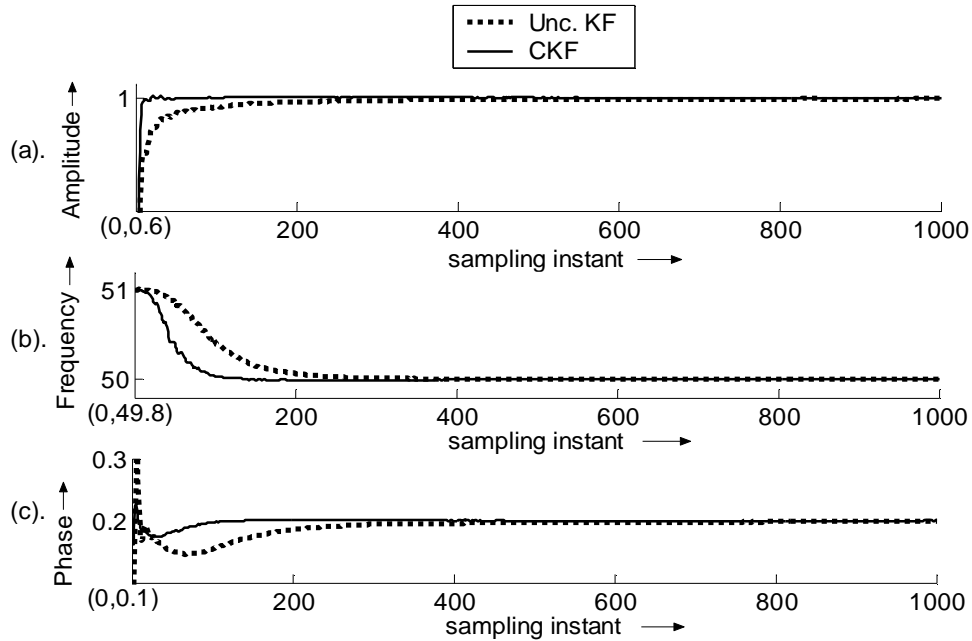


Fig. 1 Estimation results for synthetic noisy signal. (a) Estimated amplitude, (b) Estimated Frequency in Hz, and (c) Estimated Phase in radian (multiplicity factor π).

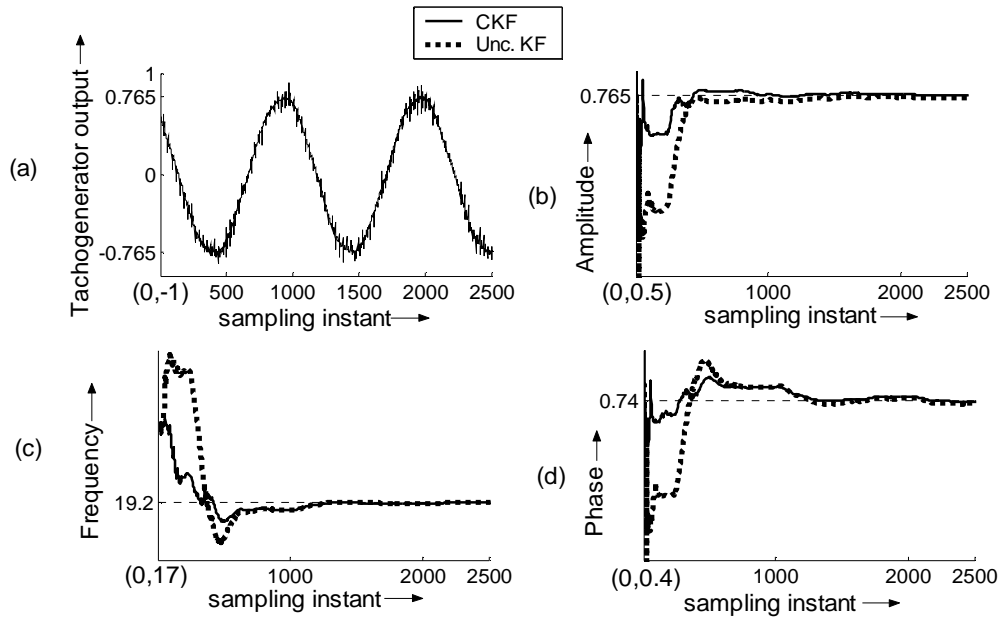


Fig. 2 Estimation results for real noisy signal. (a) Real noisy signal, (b) Estimated amplitude, (c) Estimated frequency in Hz, and (d) Estimated phase in radian.

in the lower and $\pi/2$ in the upper side. The frequency constraints are chosen to be 16 Hz in the lower side and 24 Hz in the upper side. Fig. 2 shows relatively large variations in initial estimates for unconstrained KF. During these variations, the state variable estimates may go beyond the constraints which may lead to the failure of the system or its components.

Conclusions: CKF exhibits superior performance over unconstrained KF with respect to speed of convergence and estimation accuracy. CKF takes only a few samples

to accurately estimate the state variables, whereas traditional KF takes more samples to do so. Moreover, state variable estimates satisfy the state inequality constraints thereby ensuring the estimator to converge faster. The CPU time in both the cases has been shown in Fig. 3. The computational requirement of the constrained filter is marginally higher than that of unconstrained KF. The CPU time per sample calculation has been obtained as $52\mu\text{s}$ for unconstrained KF and $54\mu\text{s}$ for CKF. These limits are well within the sampling frequency of 1 ms.

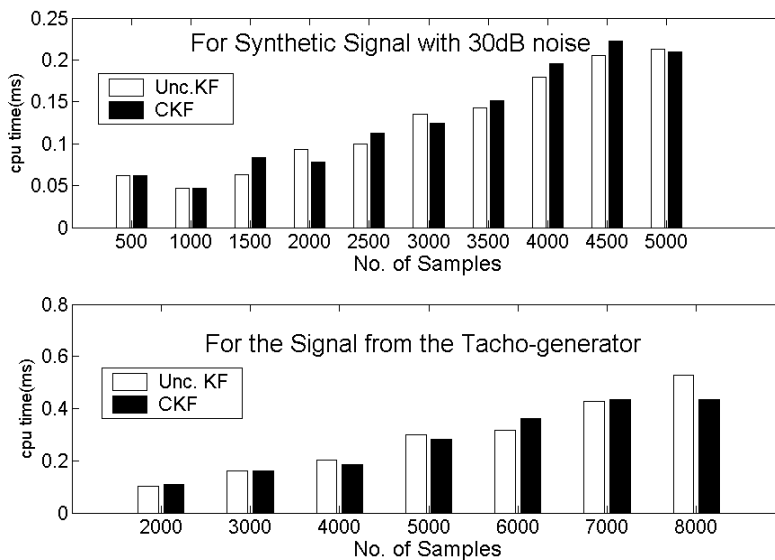


Fig. 3 CPU Time

3.3 Yawn Detection

Problem Definition: Yawn is a typical fatigue-induced event, which occurs with prolonged opening of mouth. This activity is different from other lip deformation and can be modeled as a non-rigid motion estimation problem. CKF is used to quantify the non-rigid motion patterns of lips and differentiate between yawn and other activities without being affected by the global head motion. Our objective is to detect yawn in human drivers so that fatigue induced traffic accidents can be avoided.

Design of CKF: To estimate lip motion, a finite number of initial lip contours are extracted by performing a few image processing steps and then applying snake algorithm to smoothen these contours. Suppose N is the number of such contours each having M number of pixels, which are equidistant along the contour. The dynamics of each pixel can be considered separately. Equation of motion of i^{th} pixel in k^{th} frame is given by,

$$\text{Process: } X_k = AX_{k-1} + n_{k-1} \quad (31)$$

$$\text{Measurement: } Y_k = CX_k + m_k \quad (32)$$

$$\text{where, } A = \begin{pmatrix} 1 & 0 & T & 0 \\ 0 & 1 & 0 & T \\ 0 & 0 & 1 & 0 \\ 0 & 0 & 0 & 1 \end{pmatrix} \quad X_k = \begin{pmatrix} x_k^i \\ y_k^i \\ v_{x,k}^i \\ v_{y,k}^i \end{pmatrix}$$

$$C = \begin{pmatrix} 1 & 0 & 0 & 0 \\ 0 & 1 & 0 & 0 \end{pmatrix} \quad Y_k = \begin{pmatrix} x_k^i \\ y_k^i \end{pmatrix}$$

T = time between two successive frames.

x_k^i = x-coordinate of i^{th} pixel in k^{th} frame

y_k^i = y-coordinate of i^{th} pixel in k^{th} frame

$v_{x,k}^i$ = x-component of the velocity of i^{th} pixel in k^{th} frame

$v_{y,k}^i$ = y-component of the velocity of i^{th} pixel in k^{th} frame

n_k = process noise vector

m_k = measurement noise vector

All pixels of the k^{th} frame satisfy following elliptical constraints,

$$L < \frac{x_k^i{}^2}{a_k^2} + \frac{y_k^i{}^2}{b_k^2} < H \quad (33)$$

where a_k and b_k are the lengths of the major and minor axes of the ellipse. Logarithmic barrier functions to enforce these constraints are given by,

$$g(X_k) = \log\left(\frac{x_k^i{}^2}{a_k^2} + \frac{y_k^i{}^2}{b_k^2} - L\right) + \log\left(H - \frac{x_k^i{}^2}{a_k^2} - \frac{y_k^i{}^2}{b_k^2}\right) \quad (34)$$

Following the same procedure as discussed in the previous section, we get the CKF equations as,

$$\hat{X}_k^- = A\hat{X}_{k-1} \quad (35)$$

$$P_k^- = AP_{k-1}A^T + Q \quad (36)$$

$$G_{k,unc} = P_k^- C^T (CP_k^- C^T + R)^{-1} \quad (37)$$

$$G_k = \left(I - \frac{Z_k}{t}\right) G_{k,unc} \quad (38)$$

$$\hat{X}_k = \hat{X}_k^- + G_k (Y_k - C\hat{X}_k^-) \quad (39)$$

$$P_k = (I - G_k C) P_k^- \quad (40)$$

$$\text{where, } Z_k = A \cdot \text{diag}\left(\frac{2x_k^i}{a_k^2}, \frac{2y_k^i}{b_k^2}, 0, 0\right)$$

$$A = \left(1/\left(\frac{x_k^i{}^2}{a_k^2} + \frac{y_k^i{}^2}{b_k^2} - L\right) - 1/\left(H - \frac{x_k^i{}^2}{a_k^2} - \frac{y_k^i{}^2}{b_k^2}\right)\right)$$

and all other symbols have there usual meaning.

Performance Analysis:

Data acquisition and image preprocessing: Data acquisition has been carried out using a digital camera interfaced with a desktop computer. A good temporal resolution has to be decided to extract and correlate the feature changes in an image sequence. A typical yawn can be observed if the motion of the lips is thoroughly investigated for a period of 5 to 10 seconds. In this analysis the temporal resolution is selected as 0.5 second and the video length 6 seconds. Therefore, the number of frames to be analyzed is 12. A typical image sequence of the face of a driver is shown in Fig. 4. The original images in JPEG format has been converted to gray scale images for further processing. The images require pre-processing to remove noise and find out the initial contour. Median filtering is performed for image-smoothing (Fig. 5(a) and 5(b)). The 6th frame of Fig.4 is shown in Fig. 5. Subsequently a non-linear mapping function as in (41) enhances the contrast of the image.

$$f(g_i) = \frac{1}{1 + \exp(a \times (\eta - g_i))} \quad (41)$$

In the above equation g_i is the normalized gray level of pixel. $\eta = 0.2$ invariably suppresses the gray value of low intensity area and increases the contrast so that the region of interest (mouth opening) becomes prominent. Fig. 5 (c) shows the output image for $a=10$, $\eta = 0.2$ selected on trial and error basis. Finally the image has been converted to binary form (Fig. 5 (d)). The boundary of the mouth opening is coded and the Cartesian coordinates are stored. This is the initial estimation of the probable contours in a 2-D space (Fig. 6 (a)). Once the rough contour is estimated, we define a five-by-five search area (Fig. 6 (b)) wherein we apply the snake algorithm [8] to get the optimized contour (Fig. 6 (c)).



Fig. 4 Images acquired by a digital camera. 12 frames are displayed for a typical yawn with a temporal resolution of 0.5 seconds



Fig. 5 (a) Original image in the 6th frame, (b) Output of the image using median filter. (c) Enhancement using nonlinear mapping function. (d) Binary image

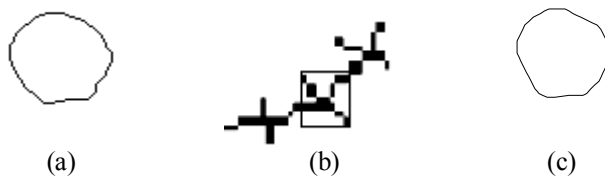


Fig. 6 (a) Boundary of mouth opening (Fig. 5 (d)), (b) Magnified search area which constrains solution contour, and (c) Optimized contour after applying snake algorithm

Lip Motion Estimation using Unconstrained KF: 64 equidistant pixels are taken for lip motion estimation and the motion of each pixel is considered separately. We have assumed that the acceleration is very small compared to other motion parameters. Therefore, acceleration is assumed to have a normal distribution and it is considered as process noise. Unconstrained KF is applied to estimate the position and velocity of the contour pixels. The estimation results are shown in Fig. 7. Fig 7 (a) shows estimated lip contours during expansion and Fig. 7 (b) shows the same during contraction. It is apparent from the result that unconstrained KF performs poor estimation because of the negligence of state variable constraints.

Lip Motion Estimation using CKF: Assuming time varying and elliptical constraints on the lip pixels, designed CKF algorithm is applied to estimate their motion. The estimated lip contours are shown in Fig 8. Fig 8(a) shows the estimated lip contour during expansion whereas Fig 8(b) shows the same during contraction. Estimation result shows that CKF performs better lip motion estimation than the traditional KF.

Yawn Detection in Human Drivers: The action units (AU) to quantify the mouth opening is measured and plotted in Fig. 9 (pixel units). The results shown are based on selected images over a period of 10 seconds with a time resolution of 0.5 seconds. The peak value of the lip opening at the time of yawn is normally four to

five times the value when the driver talks. Therefore, to detect yawn in human drivers, we keep on finding the mouth openings in terms of AU units and observe AU against frame number plot. As long as AU remains small say within 10 pixels, we say that the driver is talking to the co-passengers. As soon as a hump in the plot, with a maximum value of say 40-45 pixels over a span of 5-10 frames is noticed, we infer that the driver might have yawned. To confirm the driver's fatigue, we check the other events like eyelids movement (eyelids begin to drop as Driver starts to yawn), head motion (head may fall down frequently) etc.

Conclusions: The objective of this work is to identify the fatigue-induced behavior of human drivers by detecting the yawns. CKF has been used to detect yawn by estimating the lip motion. Constraints are nonlinear and time varying. Performance of CKF has been compared with the unconstrained KF. It has been found that CKF exhibits much better lip motion estimation with the state variable estimates satisfying the elliptical constraints in each frame. Whereas, traditional unconstrained KF gives a poor estimation because of the negligence of these constraints. Finally, from the mouth opening (AU magnitude) vs. frame number plot, we can get the information that whether the driver is yawning or talking to co-passengers.

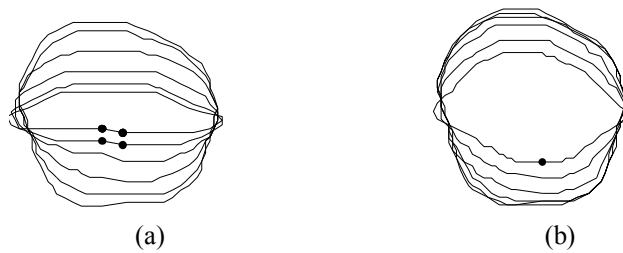


Fig 7 Estimated lip contours using unconstrained KF (a) contours during expansion and (b) contours during contraction.

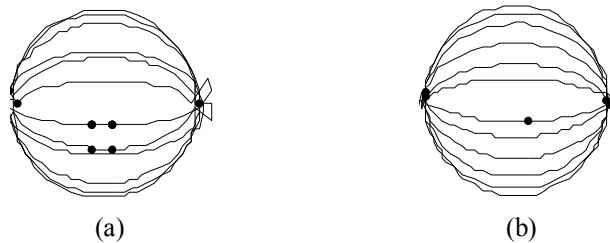


Fig 8 Estimated lip contours using CKF (a) contours during expansion and (b) contours during contraction.

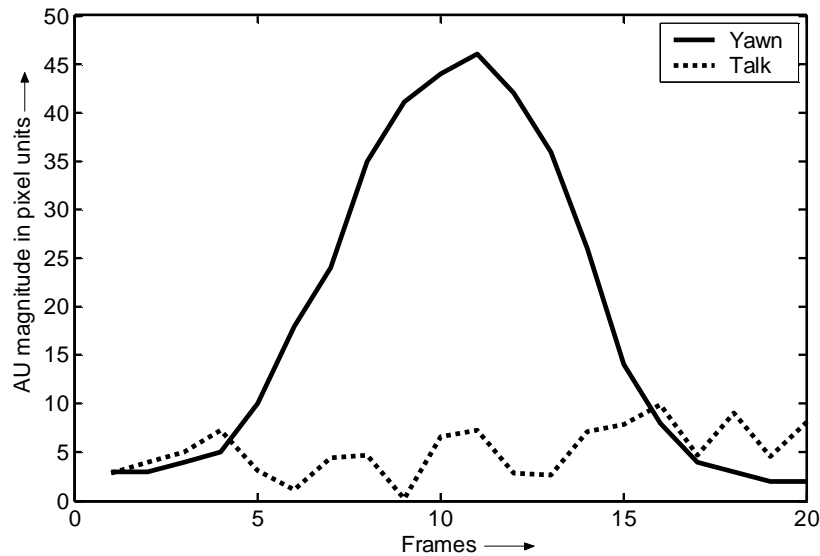


Fig. 9 AU vs. the frame sequence when the driver talks to the co-passenger (solid plot) and when the driver yawns (dotted plot).

4. References:

- [1]. Kalman, R. E., "A New Approach to Linear Filtering and Prediction Problems," *Transaction of the ASME— Journal of Basic Engineering*, pp. 35-45 (March 1960).
- [2]. W. Wen, and H. Durrant-Whyte, "Model based active object localization using multiple sensors", *Intelligent Systems and Robotics*, Osaka, Japan, (November 1991).
- [3]. W. Wen, and H. Durrant-Whyte, "Model-based multi - sensor data fusion", *IEEE International Conference on Robotics and Automation*, Nice, France, pp. 1720-1726, (May 1992).
- [4]. S. Hayward, "Constrained Kalman Filter for least-squares estimation of time - varying beam forming weights", in *Mathematics in Signal Processing IV*, (J. McWhirter and I. Proudler, Edition) Oxford University Press, pp.113-125,(1998).
- [5]. J. Porrill, "Optimal combination and constraints for geometrical sensor data", *International Journal of Robotics Research* 7(6) pp. 66-77, (December 1988).
- [6]. D. Simon and T. Chia, "Kalman Filtering with state equality constraints", *IEEE Transactions on Aerospace and Electronic Systems*, 39(1), pp. 128-136, (January 2002).
- [7]. Stephen Boyd, and Lieke Vandenberghe, "Convex Optimization", Cambridge University Press, pp. 547-553 (March 2004).
- [8]. M. Kass, A. Witkin, and D. Terzopoulos, "Snakes: Active contour models," *Int. Jr. Comp. Vision*, vol. 1, pp.321-331,(1988)